3% Silicon Steel Core Material
(Grain-Oriented Electrical Steel)
datasheet

3% (Grain-Oriented) Silicon Steel is a soft magnetic material that is best used in electrical power transformers and inductors. It has a silicon content up to 3.2 mass %, which increases the electrical resistivity and reduces eddy current losses. The magnetic properties can be enhanced during a cold rolling stage (along the length) to produce textured sheets, known as grain-oriented electrical steel. Due to its preferred crystallographic orientation, it is used primarily for non-rotating applications, i.e. transformers and inductors. Typical operating frequency of 3% Silicon Steel is 50-60 Hz (hertz). A variety of forms can be manufactured, including lamination, toroidal and C-cores, as well as glued block cores of various shapes by cutting or pressing.

Date: September 2018
Revision 0.1

Fig. 1: 3% silicon core

3% Silicon Steel core

Dimensions

Table 1: Core dimensions

Description	Symbol	Finished dimension (mm)
Width of core	A	180
Height of core	B	240
Depth of core (or cast width)	D	30
Thickness or build	E	50
Width of core window	F	80
Height of core window	G	140
Gap width	H	Minimum (cut surface to cut surface)

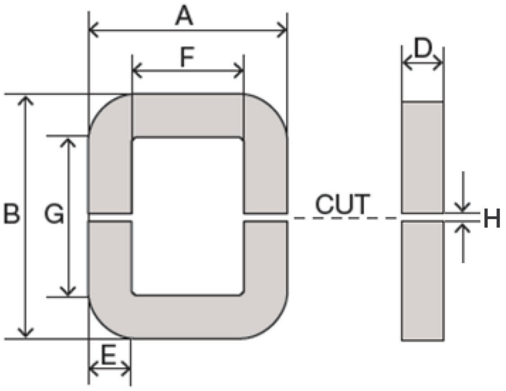

Fig. 2: Illustration of core dimensions

Acknowledgement

This technical effort was performed in support of the National Energy Technology Laboratory's ongoing research in DOE's The Office of Electricity's (OE) Transformer Resilience and Advanced Components (TRAC) program under the RES contract DE-FE0004000.

Disclaimer

NATIONAL
ENERGY
TECHNOLOGY
LABORATORY

Magnetic Characteristics

Table 2: Magnetic characteristics

Description	Symbol	Typical value	Unit
Effective area	A_e	1,425	mm^2
Mean magnetic path length[1]	L_m	583	mm
Mass (before impregnation)		6.44	kg
Mass (after impregnation)		6.78	kg
Lamination thickness		0.012 (0.305)	inch (mm)
Chemistry		$Fe_{94.2}\ Si_{5.8}$	
Grade		CRGO (cold-rolled, grain-oriented)	
Anneal		Standard – No Field	
Impregnation		50% Solids Epoxy	
Supplier		MK Magnetics	
Part number		4216AB-A	

Measurement Setup

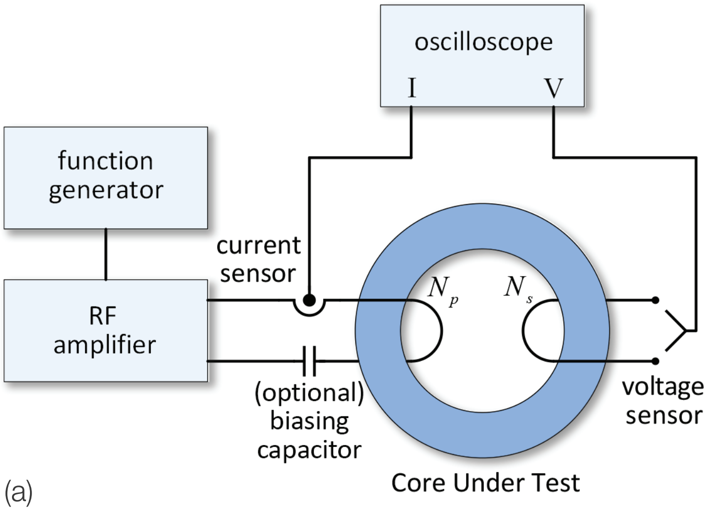

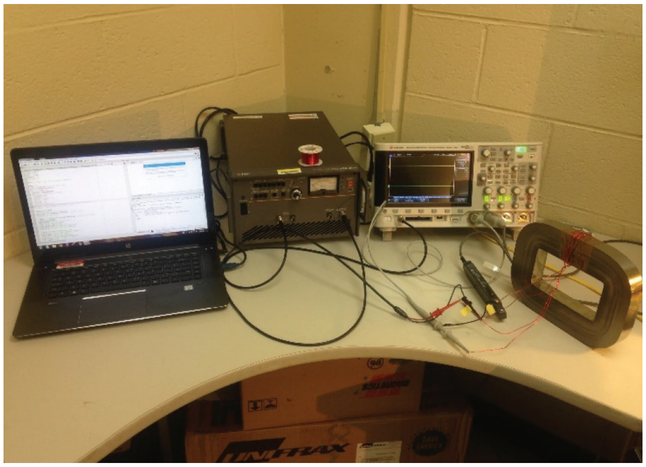

Fig. 3: Arbitrary waveform core loss test system (CLTS) (a) conceptual setup (b) actual setup

The *BH* curves, core losses, and permeability of the core under test (CUT) are measured with an arbitrary waveform core loss test system (CLTS), which is shown in Fig. 3. Arbitrary small signal sinusoidal waveforms are generated from a function generator, and the small signals are amplified via an amplifier.

---

[1] Mean magnetic path length is computed using the following equation. OD and ID are outer and inner diameters, respectively. $L_m = \dfrac{\pi(\mathrm{OD}-\mathrm{ID})}{\ln\left(\dfrac{\mathrm{OD}}{\mathrm{ID}}\right)}$

Two windings are placed around the core under test. The amplifier excites the primary winding, and the current of the primary winding is measured, in which the current information is converted to the magnetic field strengths H as

$$H(t) = \frac{N_p \cdot i(t)}{l_m} \ , \tag{1}$$

where N_p is the number of turns in the primary winding. A dc-biasing capacitor is inserted in series with the primary winding to provide zero average voltage applied to the primary winding.

The secondary winding is open, and the voltage across the secondary winding is measured, in which the voltage information is integrated to derive the flux density B as

$$B(t) = \frac{1}{N_s \cdot A_e} \int_0^T v(\tau)\, d\tau \ , \tag{2}$$

where N_s is the number of turns in the secondary winding, and T is the period of the excitation waveform.

Fig. 4 illustrates three different excitation voltage waveforms and corresponding flux density waveforms. When the excitation voltage is sinusoidal as shown in Fig. 4(a), the flux is also a sinusoidal shape. When the excitation voltage is a two-level square waveform as shown in Fig. 4(b), the flux is a sawtooth shape. The average excitation voltage is adjusted to be zero via the dc-biasing capacitor, and thus, the average flux is also zero. When the excitation voltage is a three-level square voltage as shown in Fig. 4(b), the flux is a trapezoidal shape. The duty cycle is defined as the ratio between the applied high voltage time and the period. In the sawtooth flux, the duty cycle can range from 0% to 100%. In the trapezoidal flux, the duty cycle range from 0% to 50%. At 50% duty cycles, both the sawtooth and trapezoidal waveforms become identical.

It should be noted that only limited ranges of the core loss measurements are executed due to the limitations of the amplifier, such ±75V & ±6A peak ratings and 400V/μs slew rate. The amplifier model number is HSA4014 from NF Corporation. For example, it is difficult to excite the core to high saturation level at high frequency due to limited voltage and current rating of the amplifier. Therefore, the ranges of the experimental results are limited.

Additionally, the core temperature is not closely monitored; however, the core temperature can be assumed to be near room temperature.

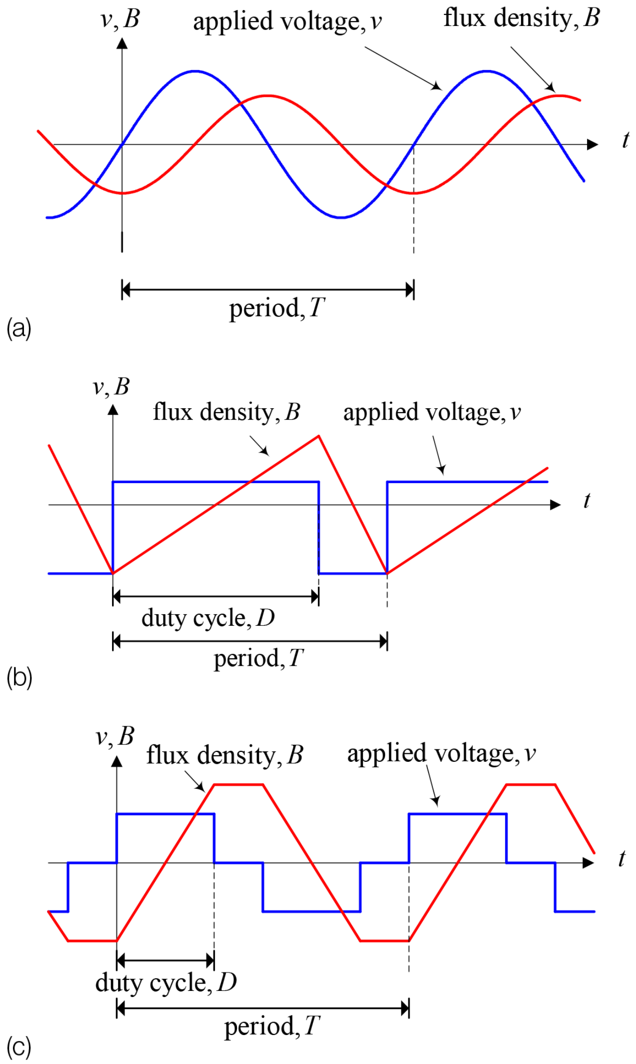

Fig. 4: Excitation voltage waveforms and corresponding flux density waveforms (a) Sinusoidal flux, (b) Sawtooth flux, and (c) Trapezoidal flux

Anhysteritic BH Curves

Fig. 5 illustrates the measured low frequency *BH* loops at 10 Hz. Using the outer most *BH* loop, the anhysteretic *BH* curve is fitted. The anhysteretic *BH* curves can be computed as a function of field intensity *H* using the follow formula.

$$
\begin{aligned}
B &= \mu_H(H)H \\
\mu_H(H) &= \mu_0 + \sum_{k=1}^{K} \frac{m_k}{h_k} \frac{1}{1+\left|H/h_k\right|^{n_k}}
\end{aligned}
\qquad (3)
$$

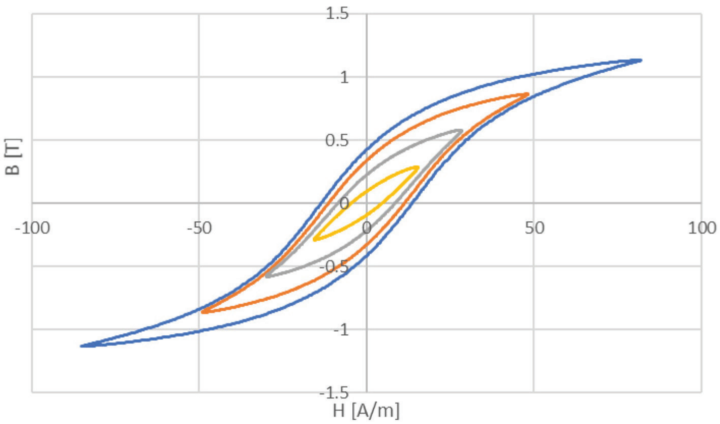

Fig. 5: Low frequency BH loops (excitation at 10 Hz, $N_p = 26$, $N_s = 26$)

Similarly, the anhysteretic *BH* curves can be computed as a function of flux density *B* using the follow formula.

$$
\begin{aligned}
B &= \mu_B(B)H \\
\mu_B(B) &= \mu_0 \frac{r(B)}{r(B)-1} \\
r(B) &= \frac{\mu_r}{\mu_r - 1} + \sum_{k=1}^{K} \alpha_k |B| + \delta_k \ln\left(\varepsilon_k + \zeta_k e^{-\beta_k |B|}\right) \\
\delta_k &= \frac{\alpha_k}{\beta_k}, \varepsilon_k = \frac{e^{-\beta_k \gamma_k}}{1+e^{-\beta_k \gamma_k}}, \zeta_k = \frac{1}{1+e^{-\beta_k \gamma_k}}
\end{aligned}
\qquad (4)
$$

Table 3 and Table 4 lists the anhysteretic curve coefficients for eqs. (3) and (4), respectively.

The core anhysteretic characteristic models in eqs. (3) and (4) are based on the following references.

> Scott D. Sudhoff, "Magnetics and Magnetic Equivalent Circuits," in *Power Magnetic Devices: A Multi-Objective Design Approach*, 1, Wiley-IEEE Press, 2014, pp.488-
>
> G. M. Shane and S. D. Sudhoff, "Refinements in Anhysteretic Characterization and Permeability Modeling," in *IEEE Transactions on Magnetics*, vol. 46, no. 11, pp. 3834-3843, Nov. 2010.

The estimation of the anhysteretic characteristic is performed using a genetic optimization program, which can be found in the following websites:

> https://engineering.purdue.edu/ECE/Research/Areas/PEDS/go_system_engineering_toolbox

Table 3: Anhysteretic curve coefficients for B as a function of H

k	1	2	3	4
m_k	1.75331805704205	-0.0906210804663391	0.194040226245213	0.191570549625740
h_k	44.5235828262732	10.9294502790288	252.485715466994	33.4444246284873
n_k	1	1.52458677140219	3.88792363656079	2.22490348042208

Table 4: Anhysteretic curve coefficients for H as a function of B

k	1	2	3	4
μ_r	30192.4844390241	0.150315028083879	-0.193972076996947	-0.269922862697259
α_k	0.507986345420917	0.0309998540777349	0.00100000000000000	0.00100000000000000
β_k	98.3104343271813	27.1444543072020	3.12127495942455	2.54436369218015
γ_k	1.75094029085722	1.69292412092536	10.0000000000000	1.97742444749062
δ_k	0.00516716611921697	0.00114203268656280	0.000320381899383951	0.000393025573770527
ε_k	1.74749179427138e-75	1.10318385629246e-20	2.78275573324989e-14	0.00648803129747218
ζ_k	1	1	0.999999999999972	0.993511968702528

Fig. 6 illustrates the measured *BH* curve and fitted anhysteretic *BH* curves as functions of *H* and *B* using the coefficients from Table 3 and Table 4. Fig. 7 and Fig. 8 illustrates the absolute relative permeability as functions of field strength *H* and flux density *B*, respectively. Fig. 9 illustrates the incremental relative permeability.

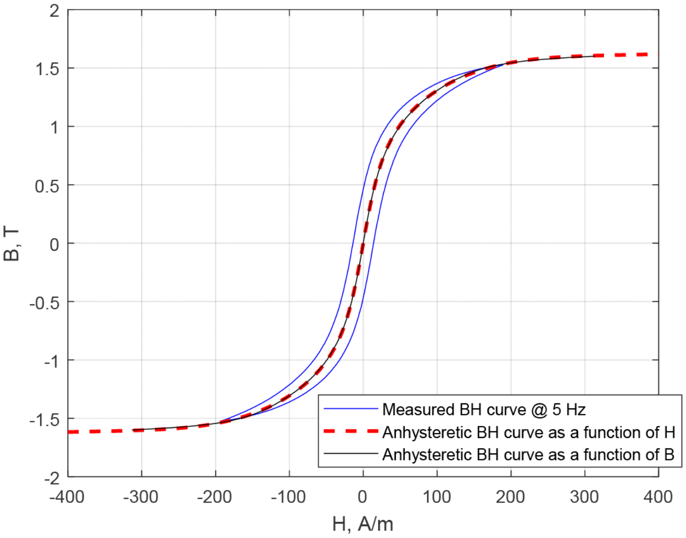

Fig. 6: Measured BH curve and fitted anhysteretic BH curve as functions of H and B

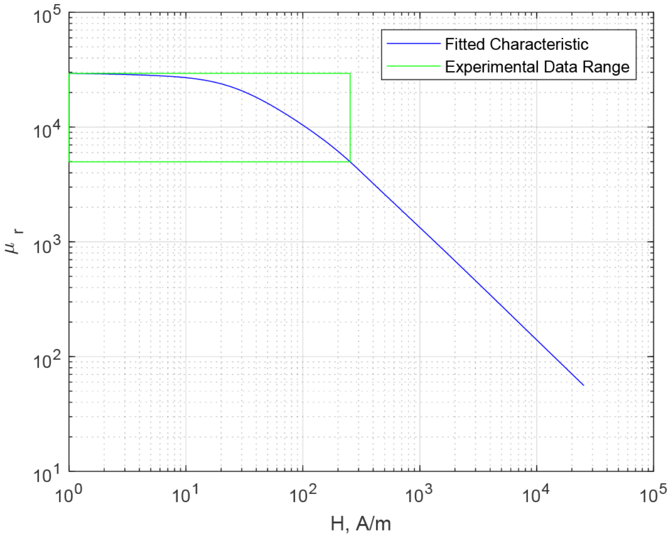

Fig. 7: Absolute relative permeability as function of field strength H

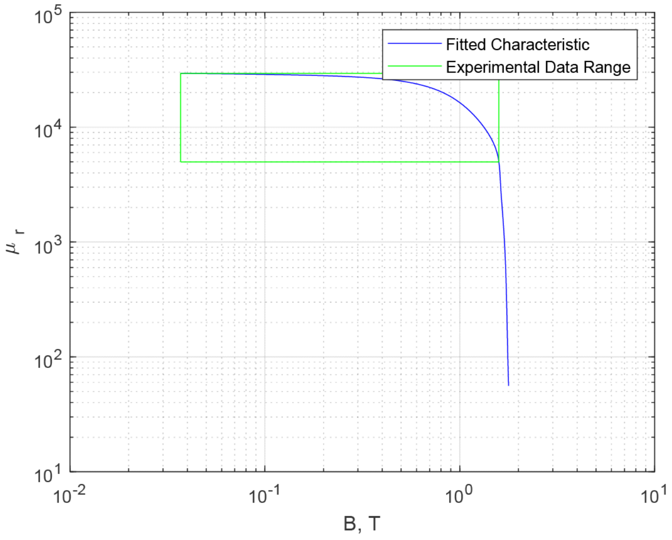

Fig. 8: Absolute relative permeability as function of flux density B

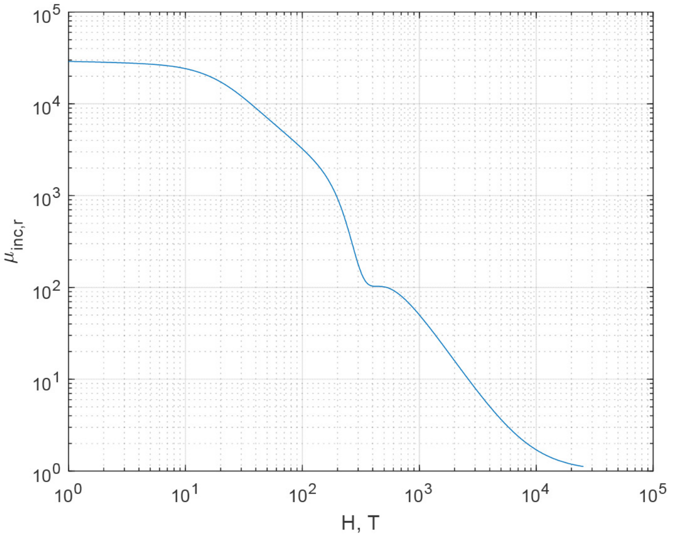

Fig. 9: Incremental relative permeability

Core Losses

Core losses at various frequencies and induction levels are measured using various excitation waveforms. Based on measurements, the coefficients of the Steinmetz's equation are estimated. The Steinmetz's equation is given as

$$P_w = k_w \cdot \left(f / f_0\right)^{\alpha} \cdot \left(B / B_0\right)^{\beta} \tag{5}$$

where P_w is the core loss per unit weight, f_0 is the base frequency, B_0 is the base flux density, and k_w, α, and β are the Steinmetz coefficients from empirical data. In the computation of P_w, the weight before impregnation in Table 2 is used, the base frequency f_0 is 1 Hz, and the base flux density B_0 is 1 Tesla.

Fig. 10 illustrates the measured *BH* curve at different frequencies. The field strength *H* is kept near constant for all frequency. At 5 Hz and 10 Hz excitations, the *BH* curve is similar, which indicates that the hysteretic losses are the dominant factor at frequencies below 5 Hz. As frequency increases, the *BH* curves become thicker, which indicates that the eddy current and anomalous losses are becoming larger.

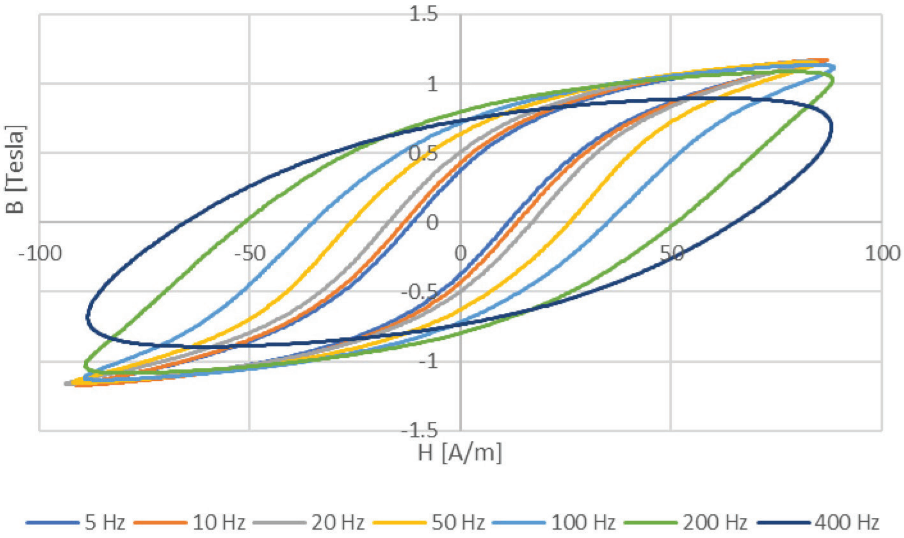

Fig. 10: BH curve as a function of frequency (N_p = 4, N_s = 4, I_p = 9.4A)

Table 5 lists the Steinmetz coefficients at different excitation conditions, and Fig. 11 illustrates the core loss measurements and estimations via Steinmetz equation.

Table 5: Steinmetz coefficients

	k_w	A	β
sine	0.000993041959535074	1.57811676723427	1.92020562967774
Sawtooth/Trapezoidal 50% duty	0.000928547094219092	1.55980765099345	1.96837844317366
Sawtooth 30% duty	0.000940705299621797	1.57628679293887	1.94124167009818
Sawtooth 10% duty	0.00137650556787012	1.60419154635983	1.91301161479668
Trapezoidal 30% duty	0.00108391002999886	1.59469005448498	1.90184381501989
Trapezoidal 10% duty	0.00161050785737820	1.64844183745327	1.84367688503077

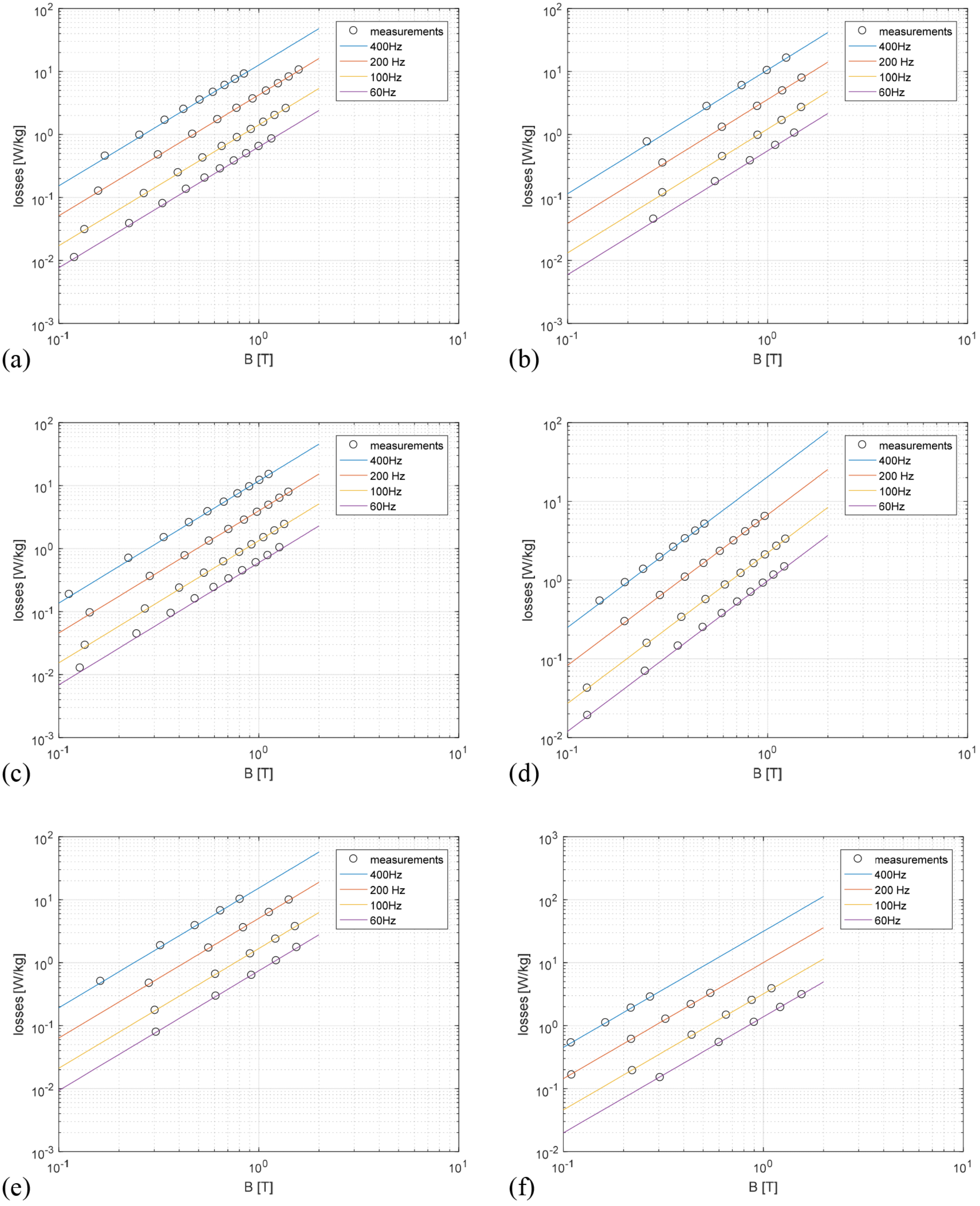

Fig. 11: Core loss measurements and estimations via Steinmetz equation: (a) Sine (b) Sawtooth/Trapezoidal 50% duty (c) Sawtooth 30% duty (d) Sawtooth 10% duty (e) Trapezoidal 30% duty (f) Trapezoidal 10% duty

Core Permeability

The permeability of the core is measured as functions of flux density and frequency. Fig. 12 illustrates the measured absolute relative permeability μ_r values, which is defined as

$$\mu_r = \frac{B_{peak}}{\mu_0 \cdot H_{peak}} \tag{6}$$

where B_{peak} and H_{peak} are the maximum flux density and field strength at each measurement point.

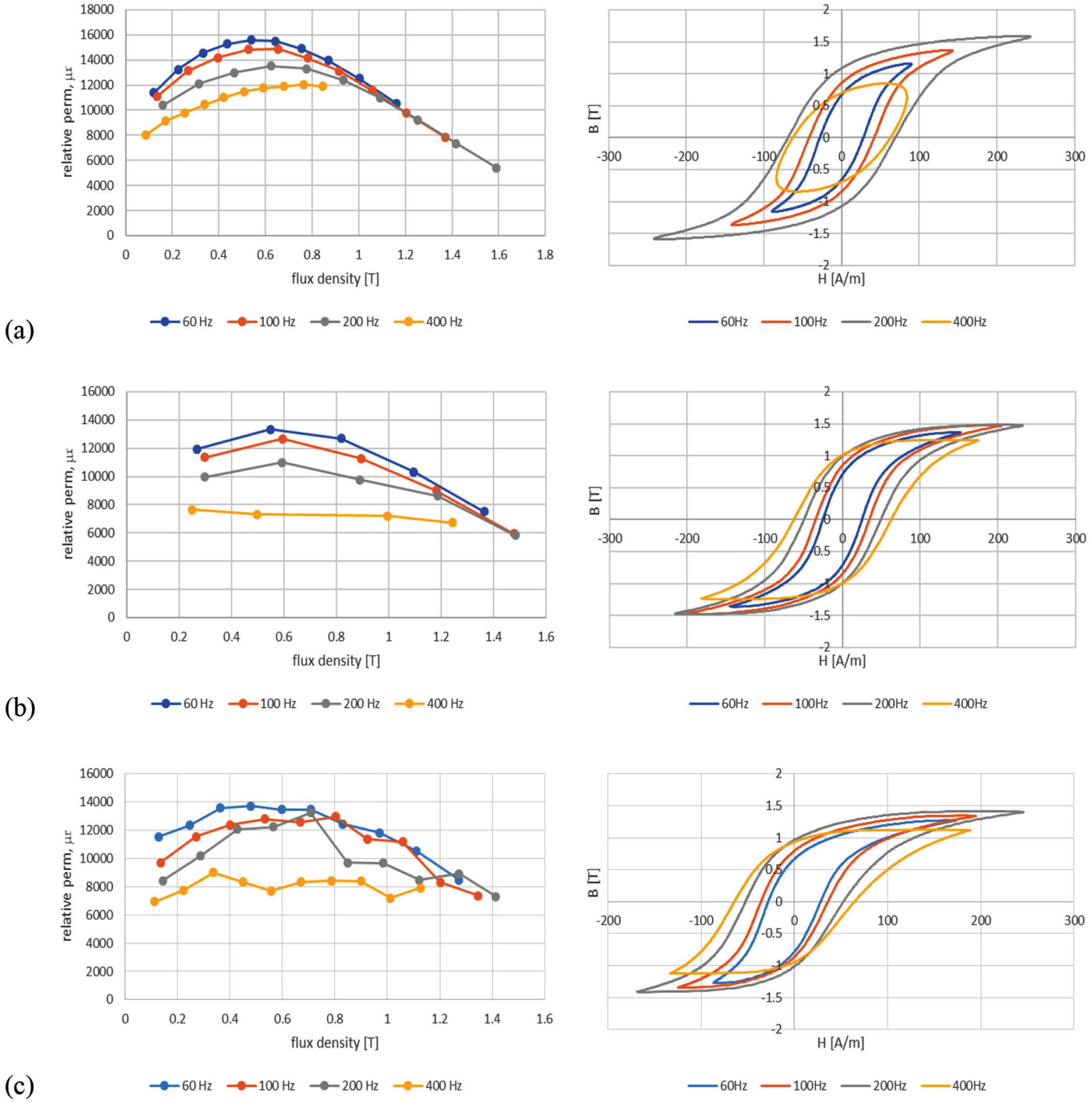

Fig. 12a: Left column: relative permeability as a function of flux density and frequency, Right column: BH loop at the maximum B of the corresponding frequency (a) Sine (b) Sawtooth/Trapezoidal 50% duty (c) Sawtooth 30% duty

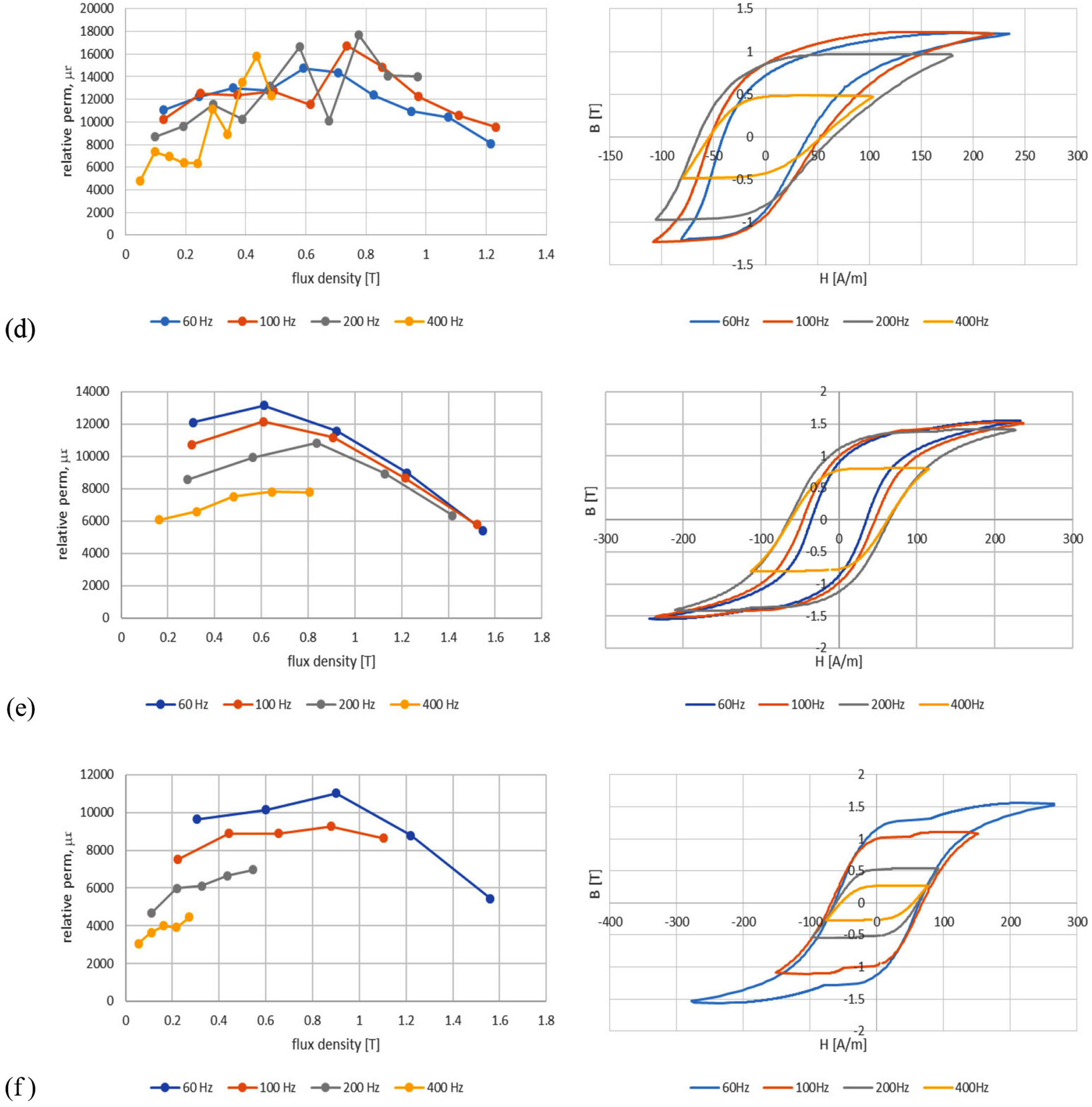

Fig. 12b: Left column: relative permeability as a function of flux density and frequency, Right column: BH loop at the maximum B of the corresponding frequency (d) Sawtooth 10% duty (e) Trapezoidal 30% duty (f) Trapezoidal 10% duty

NATIONAL
ENERGY
TECHNOLOGY
LABORATORY